

Yang Liu,^a Huihao Zhou,^{a,b,c}
Juanjuan Zhu,^a Yongxiang
Gao,^{a,b,c} Liwen Niu,^{a,b,c} Jing
Liu^{a*} and Maikun Teng^{a,b,c*}

^aSchool of Life Sciences, University of Science and Technology of China, 96 Jinzhai Road, Hefei, Anhui 230026, People's Republic of China, ^bHefei National Laboratory for Physical Sciences at Microscale, University of Science and Technology of China, 96 Jinzhai Road, Hefei, Anhui 230026, People's Republic of China, and ^cKey Laboratory of Structural Biology, Chinese Academy of Sciences, 96 Jinzhai Road, Hefei, Anhui 230026, People's Republic of China

Correspondence e-mail: jliu@ustc.edu.cn,
mkteng@ustc.edu.cn

Received 27 April 2009
Accepted 26 May 2009



© 2009 International Union of Crystallography
All rights reserved

Crystallization and preliminary crystallographic studies of the single-chain variable fragment of antibody chA21 in complex with an N-terminal fragment of ErbB2

ErbB2 is a transmembrane tyrosine kinase, the overexpression of which causes abnormality and disorder in cell signalling and leads to cell transformation. Previously, an anti-ErbB2 single-chain chimeric antibody chA21 that specifically inhibits the growth of ErbB2-overexpressing cancer cells *in vitro* and *in vivo* was developed. Here, an antibody–antigen complex consisting of the single-chain variable fragment (scFv) of chA21 and an N-terminal fragment (residues 1–192, named EP I) of the ErbB2 extracellular domain was crystallized using the sitting-drop vapour-diffusion method. An X-ray diffraction data set was collected to 2.45 Å resolution from a single flash-cooled crystal; the crystal belonged to space group $P2_12_12_1$.

1. Introduction

ErbB2 is a member of the epidermal growth-factor receptor (EGFR) family, which consists of four receptors (ErbB1–4, also known as Her1–4; Bargmann *et al.*, 1986). These four receptors all comprise an extracellular domain (ECD) with four subdomains (I/L1, II/S1, III/L2 and IV/S2), a single transmembrane domain and an intracellular tyrosine kinase domain (Burgess *et al.*, 2003). Heterodimerization or homodimerization of these receptors induces transphosphorylation on their intracellular domains and results in downstream signalling for cell proliferation and transformation (Schlessinger, 2000; Hubbard & Miller, 2007). Unlike the other three receptors, the ErbB2 ECD always maintains an extended configuration and the dimerization arm of subdomain II is well exposed for participation in the formation of homodimers or heterodimers (Cho *et al.*, 2003). This ‘autoactivated’ structure makes ErbB2 a preferred dimerization partner and its overexpression correlates with tumorigenesis and poor prognosis in breast and ovarian cancer patients (Holbro *et al.*, 2003).

Owing to the special roles of ErbB2 in tumorigenesis, it has become an attractive target for therapeutic intervention. The efficiency of using anti-ErbB2 antibodies to inhibit tumours was demonstrated in an animal model as early as 1986 (Drebin *et al.*, 1986). To date, many antibodies have been developed against ErbB2. One famous example is the humanized monoclonal antibody trastuzumab (also named Herceptin/4D5; Carter *et al.*, 2000), which was approved by the Food and Drug Administration in 1998 and is widely used in clinical therapy. Another antibody, pertuzumab (also named 2C4), is now in phase II clinical trials (Schmitz & Ferguson, 2009).

Previously, we generated an anti-ErbB2 mAb, A21, by the surface-epitope masking (SEM) method (Li *et al.*, 2003) and then constructed a single-chain chimeric antibody chA21 (scFv-Fc; Cheng *et al.*, 2003). It showed specific inhibitory activity on ErbB2-overexpressing cancer cells (Cheng *et al.*, 2003; Hu *et al.*, 2008) as well as human breast cancer xenografts (unpublished data), but the detailed anticancer mechanism of chA21 is presently unclear. According to epitope mapping, the epitope for chA21 was found to involve the first 192 residues of the N-terminus of ErbB2, a region we have named EP I (Hu *et al.*, 2008). Although the exact epitope of chA21 is unknown, it is a novel epitope that differs from those of trastuzumab and pertu-

zumab, which are located at ErbB2 ECD subdomains IV and II (Cho *et al.*, 2003; Franklin *et al.*, 2004), respectively. While the crystal structure of free chA21 scFv has been determined in previous work, here we crystallize the scFv-EP I complex in order to more clearly understand the recognition mechanism and functions of chA21.

2. Materials and methods

2.1. Protein preparation

The pGEX-4T-1 vector containing the coding sequences (CDS) of residues 1–192 of human ErbB2 (gene ID 2064) was constructed as described previously (Li *et al.*, 2005) and transformed into *Escherichia coli* Origami B. The transformed *E. coli* was cultured in Luria–Bertani media containing 100 µg ml^{−1} ampicillin at 310 K and recombinant protein expression was induced with 1 mM isopropyl β-D-1-thiogalactopyranoside (IPTG) for 20 h at 289 K. The cells were harvested and resuspended in PBS buffer (2.67 mM KCl, 1.47 mM KH₂PO₄, 138 mM NaCl and 8.10 mM Na₂HPO₄) supplemented with 0.05% (v/v) Tween-20. After pressure lysis of cells at 8.8 MPa, the cell lysates were centrifuged at 20 000g for 30 min and the supernatants were purified using glutathione–agarose (GE Healthcare). Purified GST-fusion proteins were diluted to 2 mg ml^{−1} with cleavage buffer (20 mM Tris–HCl pH 8.4, 150 mM NaCl, 2.5 mM CaCl₂) and thrombin (Novagen) was added to a final concentration of 2 U ml^{−1}. Fusion proteins were digested for 16 h at 293 K and the GST fragment was removed using glutathione–agarose. The purified EP I contains residues 1–192 of ErbB2 ECD and an additional -Gly-Ser-tag at the N-terminus.

The chimeric antibody chA21 was expressed in Chinese hamster ovary (CHO) cells cultivated in a roller-bottle incubator as described elsewhere (Cheng *et al.*, 2003; Wang *et al.*, 2005). Media containing expressed chA21 were continuously harvested every 4 d and fresh medium was added to the roller bottles. After centrifugation at 5000g for 15 min, the supernatants were successively purified using rProtein A FF (GE Healthcare) and SP-Sepharose FF (GE Healthcare). The purified chA21 was then incubated at 310 K for 5 d to autolyse into its scFv and Fc fragments. The Fc fragments were further removed by purifying again with rProtein A FF. The purified scFv contained residues 1–260 of chA21 and an additional -Ala-Ala-Asn-Pro-Ala-tag at the N-terminus, which was confirmed by mass spectroscopy and N-terminal sequencing (data not shown).

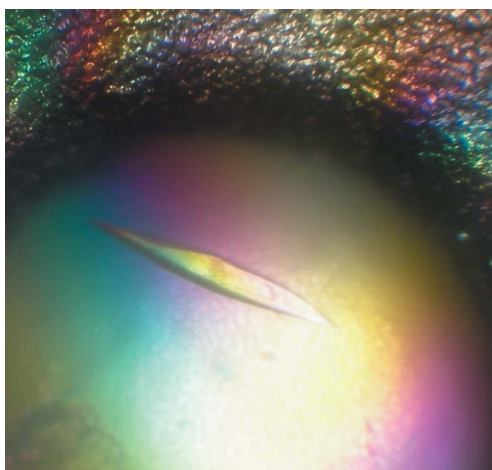


Figure 1

Photomicrograph of a crystal of the scFv-EP I complex. The dimensions of this single crystal are about 0.5 × 0.05 × 0.03 mm.

Table 1

X-ray diffraction data-collection and processing statistics.

Values in parentheses are for the last resolution shell.

| | |
|--|---|
| Space group | <i>P</i> 2 ₁ 2 ₁ 2 ₁ |
| Wavelength (Å) | 1.000 |
| Resolution (Å) | 30.0–2.45 (2.58–2.45) |
| Unit-cell parameters (Å) | <i>a</i> = 82.2, <i>b</i> = 87.2, <i>c</i> = 108.5 |
| Unique reflections | 29113 (4139) |
| Redundancy | 3.6 (3.2) |
| Completeness (%) | 99.4 (98.5) |
| Average <i>I</i> / <i>o</i> (<i>I</i>) | 9.3 (2.3) |
| <i>R</i> _{merge} [†] (%) | 7.2 (33.6) |
| No. of chA21–EP I complexes per unit cell (<i>Z</i>) | 8 |
| <i>V</i> _M (Å ³ Da ^{−1}) | 2.0 |
| Solvent content (%) | 37.8 |

[†] $R_{\text{merge}} = \sum_{hkl} \sum_i |I_i(hkl) - \langle I(hkl) \rangle| / \sum_{hkl} \sum_i I_i(hkl)$, where $I_i(hkl)$ is the *i*th observation of reflection hkl and $\langle I(hkl) \rangle$ is the average intensity for all observations *i* of reflection hkl .

Purified EP I and scFv were mixed in a molar ratio of about 1:1 and incubated at 277 K for 16 h. The complex was then purified by Superdex G75 gel-filtration chromatography (GE Healthcare) and DEAE-Sepharose (GE Healthcare). The purified complex was further desalting and concentrated to 22 mg ml^{−1} in 40 mM NaCl, 5 mM Tris–HCl pH 7.0. The protein concentration was determined using the BCA (bicinchoninic acid) protein-assay kit (Pierce) according to the user instructions. When analyzed by 10% SDS-PAGE, the purified complex showed two bands, the molecular weights of which coincided with EP I and scFv, respectively. It also showed that the molar ratio of EP I and scFv was near 1:1, with a purity of more than 95%.

2.2. Crystallization

Crystallization trials of the scFv-EP I complex were initially performed using Protein Complex Screen kits designed by Radaev *et al.* (2006). After several rounds of optimization, large single crystals (Fig. 1) that were suitable for X-ray diffraction experiments were finally obtained using the sitting-drop vapour-diffusion method with reservoir solution consisting of 15% (w/v) polyethylene glycol 4000, 100 mM 3-(1-pyridino)-1-propane sulfonate and 100 mM sodium cacodylate pH 6.5. The sitting drops, each of which consisted of 1 µl protein solution (7 mg ml^{−1}, diluted with 40 mM NaCl) and 1 µl reservoir solution, were equilibrated against 100 µl reservoir solution for 3–5 d at 295 K.

2.3. Data collection

For data collection, the crystal was removed from the crystallization drop and soaked in cryoprotectant solution [15% (w/v) polyethylene glycol 4000, 100 mM 3-(1-pyridino)-1-propane sulfonate, 100 mM sodium cacodylate pH 6.5 and 20% (v/v) glycol] for a few seconds. The crystal was then flash-cooled in a nitrogen-gas stream at 100 K. A complete diffraction data set of 99 images was collected using a single cryocooled crystal belonging to space group *P*2₁2₁ at 1.000 Å wavelength on beamline 3W1A of the Beijing Synchrotron Radiation Facility (BSRF) at the Institute of High Energy Physics, Chinese Academy of Sciences. For each image, the exposure time was 30 s and the oscillation angle was 1°. The beam size was 0.3 × 0.3 mm and the distance between the crystal and the MAR CCD detector (MAR Research) was 160 mm. The diffraction data were processed using *MOSFLM* (Leslie, 1994) and programs from the *CCP4* package (Collaborative Computational Project,

Number 4, 1994). Data-collection and processing statistics are summarized in Table 1.

3. Results and discussion

chA21 has proven to be effective in inhibiting ErbB2-overexpressing tumours *in vitro* and *in vivo*, making it a potential therapeutic antibody with high development value. In addition, it can down-regulate ErbB2 levels in ErbB2-overexpressing cancer cells (Hu *et al.*, 2008), which implies a different mechanism from those of trastuzumab and pertuzumab. Solving the crystal structure of the scFv–EP I complex will define the exact epitope of chA21 and further reveal the possible relationship between its obvious effect of down-regulating ErbB2 and the epitope. Analysis of the complex structure is also useful for humanization and affinity improvement of chA21, which is important for the development of antibody drugs.

As described above, gel-filtration chromatography was employed to purify the scFv–EP I complex from the incubated mixture of scFv and EP I. The major elution peak had an elution volume (V_e) of 56.8 ml. The Superdex 75 16/60 column (GE Healthcare) was previously calibrated with protein markers from the LMW calibration kit (GE Healthcare) and the standard curve equation was determined as $\log \text{MW} = 6.1838 - 0.02658V_e$ ($R = 0.998$). The molecular weight of the protein complex calculated using the standard curve equation was 47.2 kDa. It indicates that the scFv–EP I complex consists of one scFv (28.2 kDa from the protein sequence) and one EP I (21.6 kDa from the protein sequence), which corresponds to the expected binding of one monovalent scFv fragment one antigen molecule.

The crystal of the scFv–EP I complex belonged to the orthorhombic system, with unit-cell parameters $a = 82.2$, $b = 87.2$, $c = 108.5$ Å. Systematic absences of reflections indicated that the space group was $P2_12_12_1$. Matthews coefficient analysis suggested the presence of two scFv–EP I complexes in the asymmetric unit, which corresponds to a crystal volume per unit protein mass of $2.0 \text{ \AA}^3 \text{ Da}^{-1}$ and a solvent content of about 37.8%. The assumption that two scFv and two EP I molecules were present in the asymmetric unit was also confirmed by the recent solution of the complex structure using the molecular-replacement method with the structures of chA21 scFv (PDB code 2gjj; Hu *et al.*, 2008) and the ErbB2 extracellular domain (PDB code 2a91; Garrett *et al.*, 2003) as search models. Further refinement and analysis of the structure are under way.

We thank Professor Yuhui Dong, Professor Peng Liu and their colleagues at beamline 3W1A of BSRF for assistance during data collection. Financial support for this project was provided by grants from the National Natural Science Foundation of China (Nos. 30570362 and 30571066), the Specialized Research Fund for the Doctoral Program of Higher Education (No. 20060358021), the Chinese Ministry of Science and Technology (Nos. 2006CB806500, 2006CB910200, 2006AA02A318 and 2006AA02A245) and the Chinese Academy of Sciences (No. KSCX2-YW-R-60).

References

Bargmann, C. I., Hung, M. C. & Weinberg, R. A. (1986). *Nature (London)*, **319**, 226–230.

Burgess, A. W., Cho, H. S., Eigenbrot, C., Ferguson, K. M., Garrett, T. P., Leahy, D. J., Lemmon, M. A., Sliwkowski, M. X., Ward, C. W. & Yokoyama, S. (2003). *Mol. Cell*, **12**, 541–552.

Carter, P., Fendly, B. M., Lewis, G. D. & Sliwkowski, M. X. (2000). *Breast Dis.* **11**, 103–111.

Cheng, L. S., Liu, A. P., Yang, J. H., Dong, Y. Q., Li, L. W., Wang, J., Wang, C. C. & Liu, J. (2003). *Cell Res.* **13**, 35–48.

Cho, H. S., Mason, K., Ramyar, K. X., Stanley, A. M., Gabelli, S. B., Denney, D. W. Jr & Leahy, D. J. (2003). *Nature (London)*, **421**, 756–760.

Collaborative Computational Project, Number 4 (1994). *Acta Cryst. D50*, 760–763.

Drebin, J. A., Link, V. C., Weinberg, R. A. & Greene, M. I. (1986). *Proc. Natl. Acad. Sci. USA*, **83**, 9129–9133.

Franklin, M. C., Carey, K. D., Vajdos, F. F., Leahy, D. J., de Vos, A. M. & Sliwkowski, M. X. (2004). *Cancer Cell*, **5**, 317–328.

Garrett, T. P., McKern, N. M., Lou, M., Elleman, T. C., Adams, T. E., Lovrecz, G. O., Kofler, M., Jorissen, R. N., Nice, E. C., Burgess, A. W. & Ward, C. W. (2003). *Mol. Cell*, **11**, 495–505.

Holbro, T., Civanni, G. & Hynes, N. E. (2003). *Exp. Cell Res.* **284**, 99–110.

Hu, S., Zhu, Z., Li, L., Chang, L., Li, W., Cheng, L., Teng, M. & Liu, J. (2008). *Proteins*, **70**, 938–949.

Hubbard, S. R. & Miller, W. T. (2007). *Curr. Opin. Cell Biol.* **19**, 117–123.

Leslie, A. G. W. (1994). *MOSFLM User Guide*. MRC–LMB, Cambridge, England.

Li, L. W., Liu, H. B., Hu, S. Y., Liang, D., Cheng, L. S. & Liu, J. (2005). *Sheng Wu Gong Cheng Xue Bao*, **21**, 590–596.

Li, P., Li, Y., Li, J. Y. & Liu, J. (2003). *Cancer Lett.* **193**, 139–148.

Radaev, S., Li, S. & Sun, P. D. (2006). *Acta Cryst. D62*, 605–612.

Schlessinger, J. (2000). *Cell*, **103**, 211–225.

Schmitz, K. R. & Ferguson, K. M. (2009). *Exp. Cell Res.* **315**, 659–670.

Wang, J., Shi, Y., Liu, Y., Hu, S., Ma, J., Liu, J. & Cheng, L. (2005). *Protein Expr. Purif.* **41**, 68–76.